RESEARCH PAPER

Investigation of Follicular and Non-follicular Pathways for Polyarginine and Oleic Acid-Modified Nanoparticles

Pinaki R. Desai • Punit P. Shah • Patrick Hayden • Mandip Singh

ABSTRACT

Purpose To investigate the percutaneous permeation pathways of cell penetrating peptide modified lipid nanoparticles and oleic acid modified polymeric nanoparticles.

Methods Confocal microscopy was performed on skin cultures (EpiDermFT™) for modified and un-modified nanoparticles. Differential stripping was performed following *in vitro* skin permeation of Ibuprofen (Ibu) encapsulated nanoparticles to estimate Ibu levels in different skin layers and receiver compartment. The hair follicles (HF) were blocked and *in vitro* skin permeation of nanoparticles was then compared with unblocked HF. The surface modified nanoparticles were investigated for response on allergic contact dermatitis (ACD).

Results Surface modified nanoparticles showed a significant higher ($p < 0.05$) in fluorescence in EpiDermFT™ cultures compared to controls. The HF play less than 5% role in total nanoparticle permeation into the skin. The Ibu levels were significantly high ($p < 0.05$) for surface modified nanoparticles compared to controls. The Ibu levels in skin and receiver compartment were not significantly different when HF were open or closed. Modified nanoparticles showed significant improvement in treatment of ACD compared to solution.

Conclusions Our studies demonstrate that increased skin permeation of surface modified nanoparticles is not only dependent on a follicular pathway but also occur through non-follicular pathway(s).

ABBREVIATIONS

CLSM	confocal laser scanning microscopy
CPP	cell Penetrating Peptide
DiO-NLC	DiO-dye encapsulated NLC
DiO-NLC-R11	polyarginine-11 (R11) coated DiO-NLC
DiO-NLC-YKA	YKA coated DiO-NLC
DiO-NPS	DiO encapsulated NPS
DiO-NPS+OA (PM)	DiO-NPS with OA physical mixture
DiO-NPS-OA	OA coated DiO-NPS
DiO-Sol	DiO containing solution
DXM	dexamethasone
HF	hair follicle
Ibu	ibuprofen
Ibu-NLC	Ibu-encapsulated NLC
Ibu-NLC-R11	polyarginine-11 (R11) coated Ibu-NLC
Ibu-NLC-YKA	YKA coated Ibu-NLC
Ibu-NPS	Ibu-encapsulated NPS
Ibu-NPS+OA (PM)	Ibu-NPS with OA physical mixture
Ibu-NPS-OA	OA coated Ibu-NPS
Ibu-Sol	Ibu containing solution
NHEK	normal human epidermal keratinocyte
NLC	nano structured lipid carrier
NPS	polymeric bilayered nanoparticles
OA	oleic acid
PLGA	poly(lactic-co-glycolic acid)
SC	stratum corneum

P. R. Desai · P. P. Shah · M. Singh (✉)
College of Pharmacy and Pharmaceutical Sciences
Florida A&M University, 1520 S MLK Jr. Blvd.
Tallahassee, Florida 32307, USA
e-mail: mandip.sachdeva@famu.edu

P. Hayden
MatTek Corporation, 200 Homer Avenue
Ashland, Massachusetts 01721, USA

INTRODUCTION

From many decades, researchers who are working in the field of skin delivery have questioned the importance of drug transport through the stratum corneum (SC) *versus* the hair

follicular route. Even though, earlier work suggested that follicles play a minor role in facilitating the percutaneous drug absorption, however the results of recent investigations led to some doubts on this concept (1). The advancement in the modern techniques, such as differential stripping and laser scanning microscopy have now demonstrated that the HF can be a long-term reservoir for topical applied formulations which is similar in size to the reservoir of SC on several body sites (2).

Recently, nanoparticles are increasingly being implemented in dermatological and cosmetic products. Also many efforts have been made to use them as a carrier for drug delivery into and across the skin (3). Mainly lipids (4) and polymers (5,6) are widely being used to form the nanoparticles for the effective drug delivery systems. An evaluation and optimization of these dermatological formulations require knowledge concerning the penetration pathways of nanoparticles. Nanoparticle formulations can follow intercellular, transcellular or transappendageal pathways during skin permeation. However, the physicochemical properties and the size of the topically applied nanoparticles are decisive parameters for determining the degree and route of penetration within the skin. The penetration through the lipid domains of the SC has long been observed as the sole penetration pathway for topically applied substances, which may be also true for the nanoparticles (7). Further, there is evidence that HF act as a depot for the particulate systems and that nanoparticles can penetrate into the HF canal and hence into the follicular infundibulum where it acts as a reservoir by creating high local concentrations of the drugs.

This phenomenon can be explained by simply taking into consideration that the topically applied drugs are mainly retained in the upper layers of the SC. The reservoir of the SC is located in the uppermost cell layers of the horney layer (approximately 5 μm) compared to that HF which is usually extended deep into the tissue upto 2000 μm (8). Further, the depletion of the permeant from the SC only occurs through sebum production and hair growth, both these processes are slow. Therefore, the penetrated materials are stored approximately 10 times longer in the HF than in SC enabling sustained drug release (9).

Recently in our laboratory, we have explored the possibility of using surface modification of the nanoparticles with cell penetrating peptides (CPPs) (3,10–12) and well known penetration enhancer oleic acid (OA) (13,14) to enhance the permeation of the encapsulated drugs into the skin. Broadly, we have observed that surface modification of the nanoparticles can enhance the permeation of the encapsulated dye (DiO (11,14) and DID (12)) and drugs celecoxib (10,12), ketoprofen and spantide II (11,13,14) in vitro and in vivo. More specifically, to evaluate the effect of CPPs and OA, nanostructured lipid carrier (NLC) (10–12) and polymeric bilayered nanoparticles (NPS) (13,14) were modified with R11 and OA, respectively. We have observed that CPP

conjugated NLCs and OA modified NPS showed a significant increase in fluorescence intensity in HF and sebaceous glands (11,12,14). However, we hypothesize that the surface modified nanoparticles follow intercellular and transcellular pathways in addition to the transappendageal pathway. Thus, there is a need to use several modern techniques for quantifying intrafollicular drug delivery to investigate whether surface modified nanoparticles follow follicular or non-follicular pathways.

Over the years, a diverse array of comparative methodologies have been devised that can be used to quantify the delivery of nanoparticles into HF. In recent years, many models have been developed for this purpose including: i) skin sandwich approach (15–17); ii) approaches based on optical imaging (18,19); iii) differential stripping approach (20–22) and iv) approach to selectively block follicular orifices (23–26). Barry and co-workers devised the skin sandwich model which is an intriguing in vitro methodology that utilizes two human skin membranes, assuming that the top SC blocks the shunts in the bottom SC. However in this technique, intrafollicular fate is undermined and it is effective mostly for hydrophilic drugs only (27). Further, CLSM based techniques can investigate semi-quantitatively the distribution of topically applied fluorescent dye in different skin layers and appendageal structures. In addition, fluorescence in HF is overvalued (due to over saturation) compared to different skin layers. Thus, these techniques do not allow a direct quantification of penetration into HF. Therefore instead of excised human skin model, we have used 3-dimentional (3D) follicle free EpiDerm full thickness-400 cultures (EFT-400, Mattek Corp.) to study in vitro skin permeation and distribution studies. These human neonatal foreskin tissues were used to derived these cultures and consist of human-derived epidermal keratinocytes and fibroblasts. Also, these cultures are cultured at the air-liquid interface (ALI) and are comprised of well-differentiated SC, epidermis and dermis. On topical application of the test formulations, the distribution of fluorescence was observed in different skin layers. In addition, we have used a differential stripping technique, a combination of tape stripping and cyanoacrylate biopsies. In this technique tape stripping is applied before cyanoacrylate skin biopsies to remove the topically applied drug from the SC. Then cyanoacrylate skin biopsies were performed by applying onto the skin surface and removing it after polymerization together with corneocytes and follicular casts. Thus, it is possible to quantify drug deposition in the upper HF simply by calculating the difference in the amount of drug that is extracted by each technique. In addition, to quantify drug retention in HF, a selective blocking of HF is widely used. This technique involves artificially and selective sealing of HF openings with micro-drops of a polymer-wax adhesive mixture. This essentially creates a 'follicle-free' skin area (HF close) and thus, by comparing penetrant flux through

this with that through adjacent normal skin (HF open), it is possible to quantify appendageal drug transport.

Using many *in vitro* and *in vivo* techniques it was revealed that HF has significant importance in skin permeation process [27]. However, *in vitro* based techniques are mostly preferable due to ethical reasons. It was discovered that for percutaneous follicular permeation studies, pig ear skin is widely acceptable compared to *in vitro* excised human skin, as human skin contracts after removal [2]. Hence, the results from *in vitro* diffusion cell experiments with pig ear skin should yield similar results as excised human skin and this study was performed on the pig ear skin.

The main objective of the current study was to evaluate penetration pathways of R11 and OA modified nanoparticles into the skin. Combinations of various techniques were employed to investigate penetration pathways of NLC, NLC-R11, NPS and NPS-OA into the skin. Firstly, CLSM was used with EpiDermFT™ cultures which are follicle-free. Further, the differential stripping approach was applied to quantitatively identify the penetration of the model drug, ibuprofen (Ibu), into HF and various skin layers for different nanoparticle formulations. Finally, selectively blocking of HF was used to study the permeation profile of Ibu in receiver compartment for different nanoparticle formulations.

MATERIALS AND METHODS

Materials

Miglyol 812 was kindly gifted by Sasol Germany GmbH (Witten, Germany). Compritol 888 ATO was gifted by Gattefosse (Saint Priest, France). 1,2-Dioleoylsn- glycero-3-[[N-(5-amino-1-carboxypentyl) imidodiacetic acid) succinyl nickel salt] (DOGS-NTA-Ni) was purchased from Avanti Polar lipids (Alabaster, AL, USA). Polyoxyethylene-20 oleyl ether (Volpo-20) was a kind gift from CrodaInc (Edison, NJ, USA). The six histidine tagged polyarginine peptides (R11: RRRRRRRRRRR-6 histidine tag) and YKA peptide (YKALRISRKLAK-6 histidine tag) peptide were custom synthesized by CHI Scientific, Inc. (Maynard, MA, USA). Vivaspin centrifuge filters (Molecular weight Cut-off: 10,000 Da) were purchased from Sartorius Ltd, (Stonehouse, UK). Tetrahydrofuran, tween 80, polyvinyl alcohol (PVA), sodium bicarbonate (NaHCO$_3$), phosphate buffer saline sachets (PBS, pH 7.4), trifluoroacetic acid (TFA), Dexamethasone (DXM) and dialysis membrane (Molecular weight Cut-off: 10,000 Da, flat width of 23 mm) were purchased from Sigma-Aldrich Co (St. Louis, MO, USA). HPLC grade of acetonitrile, water and ethanol were purchased from Sigma-Aldrich Co (St. Louis, MO, USA). Ibuprofen was purchased from Spectrum chemicals and laboratory products (Gardena, CA, USA). PLGA

was purchased from PURAC biomaterials (Lincolnshire, IL, USA). Oleic acid-PEG-succinimidylglutarate ester (OA) was custom synthesized from NanocsInc (New York, NY, USA). Fluorescent DiO-dye (excitation 484 nm and emission 501 nm) was procured from Invitrogen Corp (Eugene, OR, USA). All other chemicals used in this research were of analytical grade.

Preparation and Characterization of Nanoparticles

Preparation of Nanostructured Lipid Carriers (NLC)

NLCs were prepared by using a hot melt high pressure homogenization technique as explained earlier [10,11,13]. Briefly, two phases, oil phase and aqueous phase, were prepared, heated at 85°C and mixed using high speed stirring using a Virtis Cyclone IQ2 blade type homogenizer at 20,000 rpm for 1 min. Formed pre-emulsion was then passed through a high-pressure homogenizer at 20,000 psi for 5–6 cycles (Nanodebee®, South Easton, MA, USA) to make nanoparticles. The surface of prepared Ibu-NLC was then modified by simply incubating NLCs with six histidine tagged R11 (Ibu-NLC-R11) and YKA (Ibu-NLC-YKA) at room temperature for 30 min.

Preparation of Polymeric Bilayered Nanoparticles (NPS)

NPS were made using modified emulsion solvent evaporation method [14]. Briefly, Ibu containing organic phase was mixed with water phase under high speed homogenization. To prepare bilayered nanoparticles, TPP was added to Ibu containing nanoparticle dispersion. Surface of formed Ibu-NPS was modified with OA (Ibu-NPS-OA) as earlier reported method [14]. In a similar way, a physical mixture of OA without the linker was prepared as a control and labeled as Ibu-NPS + OA (PM).

Characterization of Surface Modified Nanoparticles

The particle size and zeta potential of surface modified and un-modified nanoparticles were measured using Nicomp 380 ZLS. Entrapment efficiency and assay for Ibu in nanoparticles were investigated as described previously [10–12,14].

Permeation of Surface-Modified NLC and NPS in EpiDermFT™ Culture

As explained in [28] the *in vitro* 3-dimensional EpiDerm full thickness-400 (EFT-400, Mattek Corp.) skin cultures incubated. Medium was supplied basally, as EpiDermFT™ is grown at the ALI. For CLSM studies, fluorescent dye (DiO) encapsulated nanoparticle formulations were used. For comparison, DiO solution (DiO-Sol) was prepared similarly

as explained for Ibu-Sol. 50 µl of solution and nanoparticle formulations were applied topically and carefully spread on the surface of the EpiDermFT™ culture area. Tissues were then incubated at 37°C. After 16 h, the cultures and medium were collected. Skin cultures were washed immediately with Dulbecco's phosphated buffered saline (Mattek Corporation, Ashland, MA, USA) for 30 min. The skin cultures were then fixed on the cryotome stage (Shandon Scientific Ltd, England) using cyromatrix (Thermo Scientific, Rochester, NY, USA) to collect thin transverse sections. The culture sections were then observed under CLSM (Leica Microsystems Inc, Buffalo Grove, IL, USA) similarly as (14). The Digital image software (Museum of Science, Boston, MA, USA) was used to calculate the percent fluorescence intensity of the collected images. Finally, the collected culture medium was further used to evaluate fluorescence intensity using a Tecan microplate reader.

In Vitro Skin Permeation and Distribution Studies

Preparation of Skin

Porcine ears (Yorkshire marine pigs, male, weighing about 200 lb) were obtained from a local slaughterhouse (Limestone Meat House, Monticello, FL, USA). After cleaning under cold running water, full thickness dorsal/external skin from the pig ear was removed carefully from the underlying cartilage using a scalpel, stored and used to investigate the penetration pathways of surface modified nanoparticles in the skin. The storage conditions were previously optimized by our laboratory (10–12,14). These conditions are 10% w/w glycerol in saline at −80°C for 1 week. Prior to use, the skin was rinsed in PBS (pH 7.4) for 30 min.

In Vitro Skin Permeation

The *in vitro* skin permeation studies on pig ear skin for 24 h under unocclusive conditions were performed as described previously (10–12,14). Briefly, the full thickness pig ear skin was mounted on Franz diffusion cells (Permegear Inc., Riegelsville, PA, USA). Then, 100 µl of surface modified and un-modified nanoparticle formulations including Ibu-NLC, Ibu-NLC-R11, Ibu-NLC-YKA, Ibu-NPS, Ibu-NPS-OA and Ibu-NPS + OA (PM) were applied on the diffusional surface of the skin. These sets were repeated for two types of studies: 1) differential stripping studies and 2) selective blocking of HF studies. The receiver compartment was filled with PBS (pH 7.4) containing 0.1% volpo-20. As a control Ibu solution (1 mg/ml) was prepared in polyethylene glycol (PEG 400) containing 10%v/v ethanol and 2.4%w/v Tween 80 (12). The receiver fluid was collected and analyzed by HPLC. For the skin collection, the excess formulation was removed and the skin was then washed with 50%v/

v ethanol. The entire dosing area (0.636 cm^2) was collected with a biopsy punch. The collected skin was then used for further studies.

Differential Stripping Approach

At the end of 24 h, differential stripping was carried out with the collected skin sample to determine the importance of follicular transport in CPP and OA mediated drug delivery in skin. Tape stripping was performed to collect the SC (12). Adhesive tape Transpore™ strips (3 M, St. Paul, MN, USA) were pressed onto the skin using a roller, in order to stretch the skin surface to avoid influence of furrows and wrinkles. About 10 stripes were applied one after other and were removed quickly and collected. Following tape stripping, cyanoacrylate superglue (Loctite Super Glue, Avon, OH, USA) was applied onto the dosing area and using tape strip it was removed. It was described previously that the collected tape strip with superglue may contain follicular casts and corneocytes (21). Hence, by combining these two techniques, it is possible to quantify drug deposition in the upper HF. After strip collection, the dosing area (0.636 cm^2) was punched and cut into small pieces. The collected SC, HF and remaining skin (Epi+Derm) were subjected to Ibu extraction.

Selectively Blocking Hair Follicles

The follicular closing technique (23–26,29) was performed to study the total permeation of Ibu from the modified and un-modified nanoparticles. In this technique, each HF opening was blocked with a micro-drop of varnish-wax mixture. The drop of varnish-wax mixture was placed near HF opening using 1 ml syringe containing blunt 30 gauge needle and a magnifying glass. Using metal cutter, the sharp tip of the needle was cut off. After the varnish-wax mixture dried, the skin was used for permeation. The HF blocked (close) and un-blocked (open) skin tissues were placed in between donor and receiver compartments and *in vitro* skin permeation was performed for 24 h as explained earlier. First, DiO dye containing solution was applied on the HF open and HF close skin tissues, cryo-sectioning was performed as explained earlier and 0–40 µm vertical skin sections (top skin section) were observed under CLSM. The Ibu containing nanoparticulate formulations were then applied and the drug levels in the HF open and close skin parts and in the receiver fluid was studied.

Drug Extraction from the Skin

In case of differential stripping, collected SC, HF and Epi+Derm were cut into small pieces and collected into centrifuge tubes. For selectively blocking HF studies, the collected skin was minced

into small pieces and collected in centrifuge tubes. Ibu was extracted from the skin using previously established method (10,11,13,14) and the extracts were analyzed using HPLC.

In Vitro Drug Release from Nanoparticles

In vitro drug release studies of Ibu-NLC, Ibu-NLC-R11 and Ibu-NPS, Ibu-NPS-OA were carried out using porous membrane and Franz diffusion cells (11,14). The surface modified and un-modified nanoparticle dispersions were applied on the surface of the membrane. The receiver compartment was filled with 0.1%w/v volpo in PBS (pH 7.4). The receiver compartment samples were collected after 1, 2, 4, 6, 8, 12, 22, 24, 48 and 72 h. In the end, release of Ibu from NLC and NPS was assessed using HPLC.

HPLC Analysis

Previously reported HPLC method for ketoprofen was used to analyze Ibu from the samples (11,13,14). The Ibu standard stock solution was prepared as explained in (10) for celecoxib. All injections were performed at room temperature.

Cytotoxicity of Nanoparticles

The normal human epidermal keratinocyte (NHEK) cells were obtained from the Invitrogen (Eugene, OR, USA). Primary cultures were initiated and maintained in a keratinocyte serum-free medium, EpiLife® (GIBCO, Invitrogen Corp., Carlsbad, CA, USA). The medium was supplemented with Epilife® Defined Growth Supplement (EDGS) as per manufacturer's protocol. The flasks and 96 well plates were coated with coating matrix (Invitrogen, Eugene, OR, USA) 30 min prior to use. The cells were plated in 96 well micro titer plates, at a density of 1×10^4 cells/well, allowed to incubate overnight and were treated with 100 µl of various nanoparticle formulations (without drug), diluted in cell growth medium. The cells were then incubated for 24 h at $37 \pm 0.2°C$ in a 5% CO_2-water-jacketed incubator. Cell viability in each treatment group was determined by crystal violet dye assay, described by Chougule *et al.* (30)

In Vivo Model for Allergic Contact Dermatitis (ACD)

The *in vivo* studies were carried out using ACD mouse model developed in our laboratory and reported earlier (10,11,13,14). The left ears of the treatment group of the mice were treated with the placebo formulations (without drug) and served as an internal control to study the anti-inflammatory effects of the formulation excipients. The ear thickness was assessed using a vernier caliper (Fraction +Digital Fractional Caliper, General Tools & Instruments Co., LLC., New York City, NY, USA) at 0, 24, 48 and 72 h. Right ears of the mice were treated with topical application of 50 µl of Ibu-Sol, Ibu-NLC-R11 and Ibu-NPS-OA, 2 h after antigen challenge and 3 times a day thereafter for 3 days. Dexamethasone (DXM), 0.5 mM solution was prepared and used as a positive control (14). The ear swelling for treatment group was performed as reported in (14). The histological examination of the ears was performed as explained in (10).

Statistics

Data were expressed as the means and standard deviation (mean ± SD). Using GraphPad PRISM version 5.0 software (La Jolla, CA, USA), One-way ANOVA followed by Tukey's Multiple Comparison Test was performed to aseess the significance of differences among test groups. Differences were considered to be significant at $p < 0.05$.

RESULTS

Characterization of Nanocarrier Systems

The mean particle size of NLC and NLC-R11 was found to be 140 ± 16 nm and 143 ± 9 nm, respectively with polydispersity indices (PI) of 0.18 ± 0.03 and 0.16 ± 0.08. The zeta potential of NLCs was -16.62 ± 3.16 mV, which was decreased to -7.36 ± 2.93 mV after surface modification of NLC with R11. The prepared Ibu-NLC showed about 95–97% of encapsulation efficiencies. The total (bound and unbound) Ibu present in NLC dispersion was 0.85 ± 0.02 mg/ml. Further, the particle size of formed NPS was 181 ± 16 nm and was increased with OA surface modification and was found to be 195 ± 15 nm. The PI of NPS and NPS-OA were 0.24 ± 0.06 and 0.26 ± 0.09, respectively. The zeta potential of NPS in double distilled water was 12.52 ± 4.03 mV and further decreased to 7.83 ± 3.54 mV for NPS-OA. The entrapment efficiency of Ibu in Ibu-NPS was $94.53 \pm 1.71\%$ and it was unaffected by surface modification. The total Ibu present in NPS dispersion was found to be 0.81 ± 0.09 mg/ml.

Permeation of Surface Modified NLC and NPS in EpiDermFT™ Culture

The results from *in vitro* tracking of surface modified and unmodified NLC and NPS in EpiDermFT™ cultures are summarized in Fig. 1. Cultures showed intense fluorescence in SC for DiO-NLC, DiO-NLC-YKA and DiO-NPS (Fig. 1a). Fluorescence was not observed in the epidermis or dermis layer. However, the fluorescence from DiO-NLC-
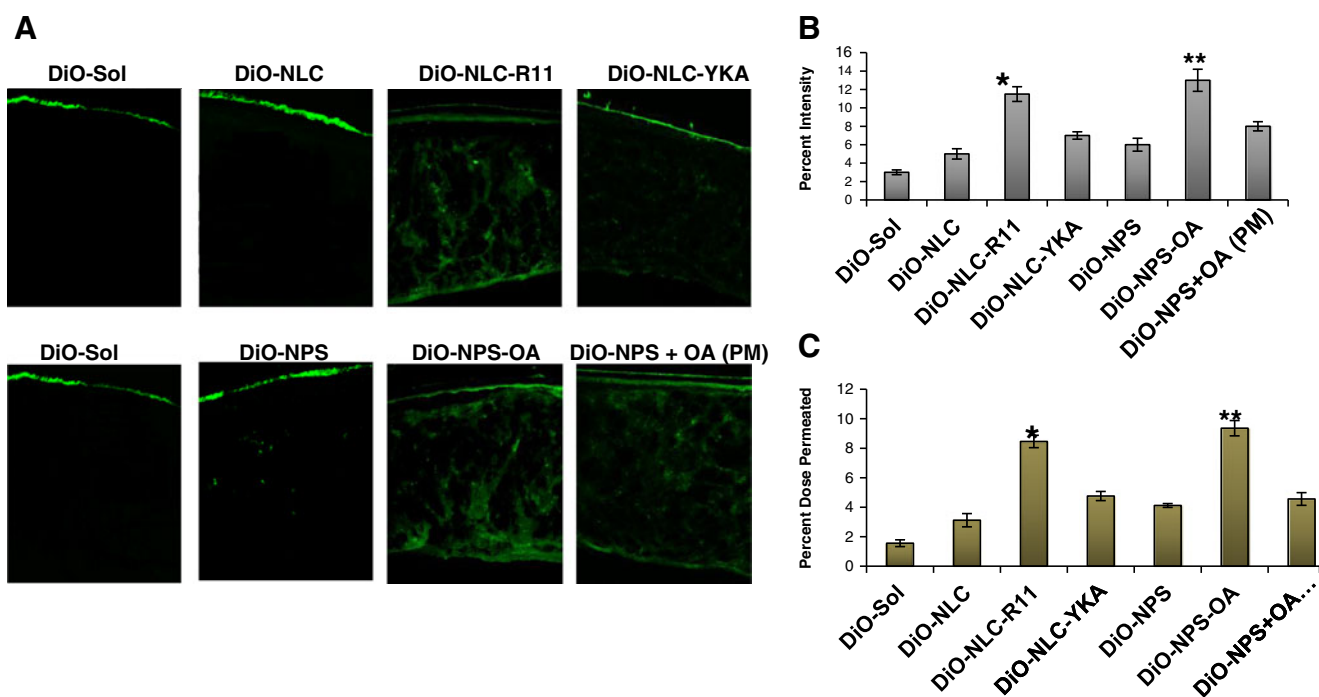
A

B

C

Fig. 1 EpiDermFT™ permeation & confocal imaging: (**a**) *in vitro* EpiDermFT™ permeation of DiO encapsulated modified and un-modified nanoparticles with DiO-Sol. 16 h following application of the indicated nanoparticles, the full thickness skin equivalent sections were cut with a cryotome and observed with a CLSM for associated fluorescence. The top row indicates the NLC formulations and bottom row indicates the NPS formulations. (**b**) comparison between the percent fluorescence intensity of the DiO encapsulated surface modified and un-modified nanoparticles for permeated skin equivalent sections; (**c**) comparison between the fluorescence intensity of the collected medium. Data represent mean $\pm$ SD ($n = 6$); significance DiO-NLC-R11 against DiO-Sol, DiO-NLC and DiO-NLC-YKA, $*p < 0.05$; significance DiO-NPS-OA against DiO-Sol, DiO-NPS and DiO-NPS + OA (PM), $**p < 0.05$.

R11 and DiO-NPS-OA treated cultures showed uniform distribution throughout the skin layers. Further, the percent fluorescence intensity, calculated from confocal microscopic images, was in the range between 0 and 13 for the entire section (Fig. 1b). The percent intensity of DiO-NLC-R11 was significantly higher ($*p < 0.05$) than DiO-Sol, DiO-NLC and DiO-NLC-YKA. Similarly, DiO-NPS-OA showed significantly higher ($**p < 0.05$) percent intensity than DiO-Sol, DiO-NPS and DiO-NPS + OA (PM). Increased permeation was observed for DiO-NPS + OA (PM) treated cultures but the total intensity was significantly less compare to DiO-NPS-OA. In addition, the medium collected from DiO-NLC-R11 and DiO-NPS-OA treated cultures showed significant increases ($p < 0.05$) in the dye permeation compared to controls (Fig. 1c). This observation confirms that surface modification plays a vital role in increasing skin permeation of encapsulated drugs and the permeation can occur via intercellular and transcellular permeation pathways as EpiDermFT™ cultures do not contain HF.

Differential Stripping Approach

The results of the present investigation show that after 24 h of skin permeation, Ibu encapsulated nanoparticles can penetrate into the HF. Using differential stripping, Ibu levels in different parts of the skin, including HF, SC, Epi + Derm was studied effectively and the results are presented in Fig. 2. The levels in the HF reservoir varied with the different formulations; these levels were 0.29 ± 0.01 µg; 0.69 ± 0.078 µg; 0.94 ± 0.096 µg and 0.62 ± 0.079 µg for Ibu-Sol; Ibu-NLC; Ibu-NLC-R11 and Ibu-NLC-YKA, respectively (Fig. 2a). Further, the levels of Ibu in SC, Epi + Derm were significantly increased ($*p < 0.05$) for Ibu-NLC-R11 (Fig. 2a). The levels of Ibu penetrated into HF for the formulations: Ibu-NPS; Ibu-NPS-OA and Ibu-NPS + OA (PM) were 0.77 ± 0.034 µg; 1.07 ± 0.092 µg and 0.82 ± 0.047 µg, respectively (Fig. 2b). The SC and Epi + Derm retention of Ibu from Ibu-NPS-OA was 4.06 ± 029 and 16.73 ± 0.36, respectively and these values were significantly increased compared to the other polymeric nanoparticle formulations. The amount of Ibu permeated into the receiver compartment after 24 h from NLC formulations is summarized in Fig. 3a and from NPS formulations in Fig. 3b. The amount of Ibu from Ibu-NLC-R11 permeated into the receiver compartment was 13.85 ± 0.82 µg/cm^2. This amount was 4.3; 2.2 and 1.7 times higher than Ibu-Sol; Ibu-NLC and Ibu-NLC-YKA, respectively (Fig. 3a). As shown in Fig. 3b, the amount of Ibu permeated into receiver compartment from Ibu-NPS-OA
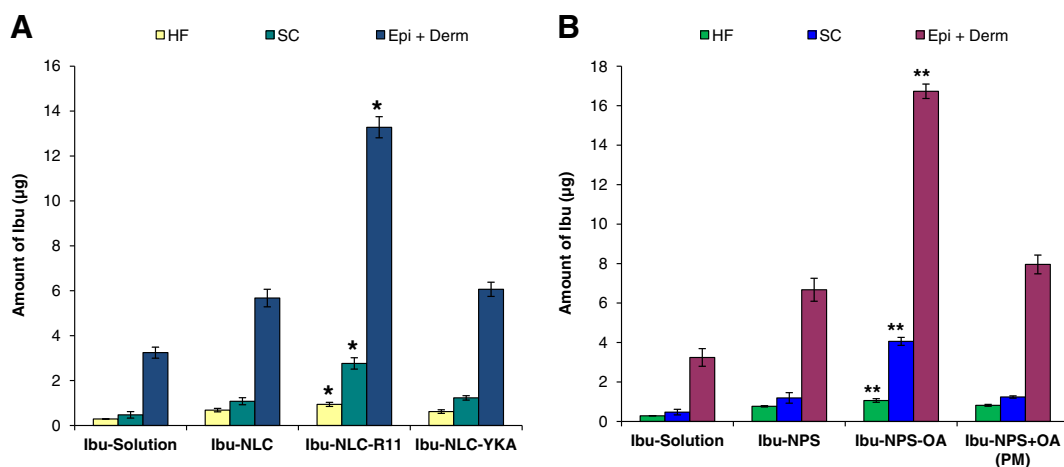
Fig. 2 Differential stripping approach - Distribution of Ibu in the skin: *In vitro* pig ear skin permeation of surface modified and un-modified nanoparticles (**a**) lipid nanoparticles: Ibu-NLC Ibu-NLC-R11 and Ibu-NLC-YKA; (**b**) polymeric nanoparticles: Ibu-NPS Ibu-NPS-OA and Ibu-NPS + OA (PM). Permeation was performed for 24 h was performed on Franz diffusion cells. After permeation, adhesive tape stripping and cyanoacrylate surface biopsies was performed to quantify the Ibu levels in stratum corneum (SC), hair follicle (HF) and remaining skin layers (Epi + Derm). Data represent mean ± SD, $n = 6$, significance Ibu-NLC-R11 against Ibu-Sol, Ibu-NLC and Ibu-NLC-YKA, *$p < 0.05$; significance Ibu-NPS-OA against Ibu-Sol, Ibu-NPS and Ibu-NPS + OA (PM), **$p < 0.05$.

was significantly higher (**$p < 0.05$) than Ibu-Sol, Ibu-NPS and Ibu-NPS + OA (PM).

Selectively Blocking Hair Follicles

In Vitro Skin Permeation of DiO-Dye Nanoparticles

The first aim for the selectively blocking HF studies was to effectively close the HF orifice and thus, CLSM technique was selected to visualize the orifice. It was observed that HF acts as a relevant reservoir and one of the potential skin penetration pathways for DiO-Sol (Fig. 4a and b). The application of a micro-drop of varnish-wax mixture on the

HF orifice of pig ear skin resulted in the artificial closing of the HF (Fig. 4c and d). In the previous experiments, it was demonstrated that application of the varnish-wax mixture can block the HF openings, this artificial blocking of the HF orifice ensures that they were excluded from the drug penetration.

In Vitro Skin Permeation of Ibuprofen Nanoparticles

The amount of Ibu retained in the skin following topical application of Ibu-Sol, Ibu-NLC and Ibu-NLC-YKA differed for opened HF than and closed HF (Fig. 5a). For the tested formulations, more Ibu was detected in the skin with
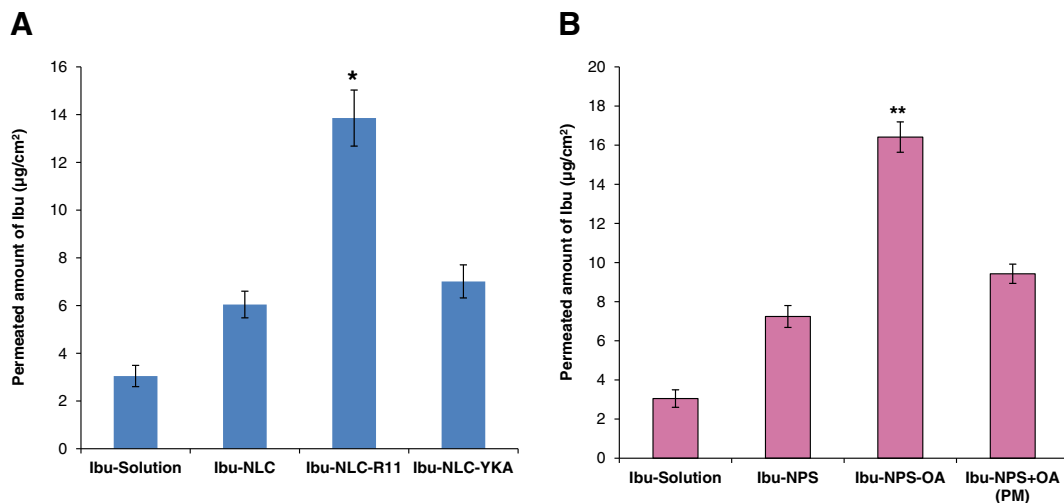

Fig. 3 Differential stripping approach – Perpetration of Ibu through the skin: *In vitro* pig ear skin permeation of surface modified and un-modified nanoparticles (**a**) lipid nanoparticles: Ibu-NLC Ibu-NLC-R11and Ibu-NLC-YKA; (**b**) polymeric nanoparticles: Ibu-NPS Ibu-NPS-OA and Ibu-NPS + OA (PM). Permeation was performed for 24 h was performed on Franz diffusion cells. After permeation, the Ibu level in receiver compartment was determined using HPLC. Data represent mean ± SD, $n = 12$, significance Ibu-NLC-R11 against Ibu-Sol, Ibu-NLC and Ibu-NLC-YKA, *$p < 0.05$; significance Ibu-NPS-OA against Ibu-Sol, Ibu-NPS and Ibu-NPS + OA (PM), **$p < 0.05$.

Fig. 4 Selective blocking of HF using a microdrop of varnish-wax mixture: Following blocking of HF, DiO-Sol was applied to the pig ear skin and the sections were collected 24 h after application. The top panel represents HF Open: (**a**) Bright Field, (**b**) Green Fluorescence Field; and the bottom panel represent HF Close skin: (**c**) Bright Field; (**d**) Green Fluorescence Field.
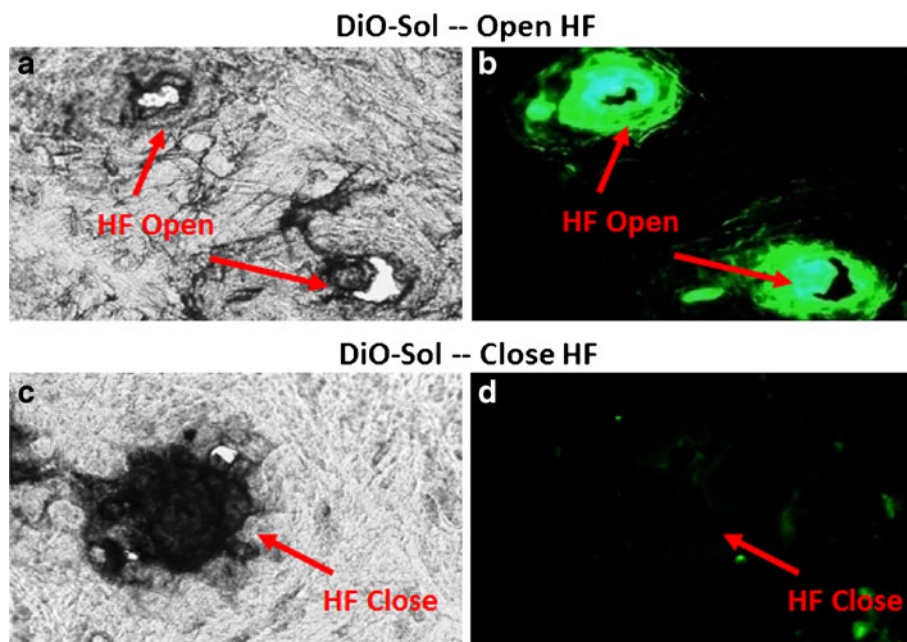
the open HF (control skin) compared to closed HF (test skin). The amount of Ibu retained in the total skin from Ibu-NLC-R11 was 14.54 ± 0.317 µg when HF were closed. However it was increased to 15.97 ± 0.46 µg when HF were open (Fig. 5a), indicating involvement of the intercellular and intracellular pathways for R11 mediated drug delivery into the skin. As observed in differential stripping experiments, in both conditions (HF open or close) Ibu levels in the skin from Ibu-NLC-R11 was significantly higher (*$p < 0.05$) compared to Ibu-Sol, Ibu-NLC and Ibu-NLC-YKA.

Further, the levels of Ibu retained in the skin from Ibu-NPS-OA for HF open (control skin) was 15.29 ± 0.52 µg and was 16.85 ± 0.62 µg for HF close (Fig. 5b). The artificial closing of the HF orifice reduced the amount of Ibu retained in the skin after application of Ibu-NPS-OA treated skin samples insignificantly. However, the amount of Ibu in the skin from Ibu-Sol, Ibu-NPS and Ibu-NPS + OA (PM) was not significantly affected by artificial blockage of the HF (Fig. 5b). The levels of Ibu from Ibu-NPS-OA was significantly higher (**$p < 0.05$) in both the cases (HF open or close) compared to Ibu-Sol, Ibu-NPS and Ibu-NPS + OA (PM).

For NLC-R11, the amount of Ibu permeated in the receiver compartment was found to be 12.24 ± 0.81 µg/cm^2 when HF were closed. This level was increased to
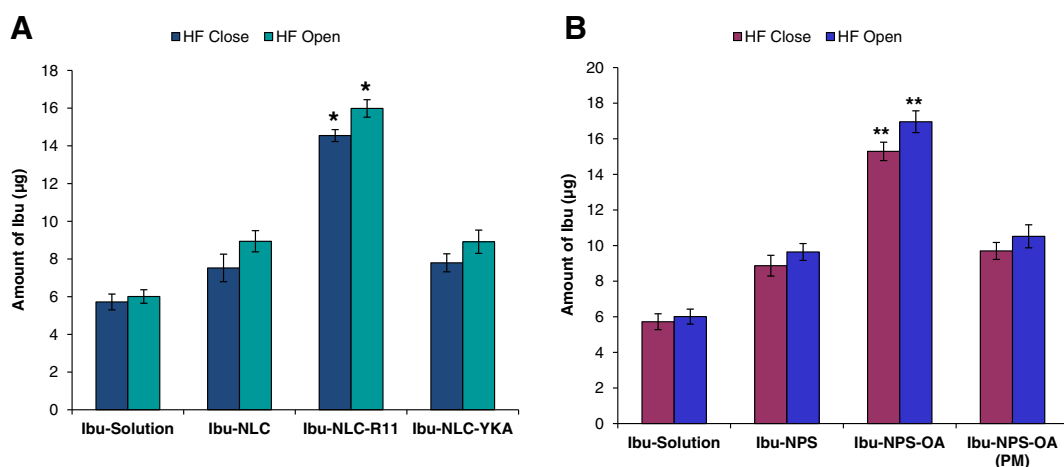

Fig. 5 Selective blocking of HF - Distribution of Ibu in the skin: The HF blocked and un-blocked test area of skin was evaluated for *in vitro* skin permeation for CPP and OA surface modified nanoparticles. The skin biopsies were collected and tested for retention of Ibu in skin layers. The Ibu levels at the end of 24 h (**a**) when applied in a form of CPP surface modified NLC and (**b**) when applied as a form of OA surface modified NPS. Data represent mean $\pm$ SD, $n = 6$, significance Ibu-NLC-R11 against Ibu-Sol, Ibu-NLC and Ibu-NLC-YKA, *$p < 0.05$; significance Ibu-NPS-OA against Ibu-Sol, Ibu-NPS and Ibu-NPS + OA (PM), **$p < 0.05$.

13.85 ± 0.82 µg/cm^2 when HF were open, however the increase was not significant (Fig. 6a). Similar to R11, OA also showed that the amount of Ibu permeated into the receiver compartment was not affected by artificial HF closure. Moreover, the Ibu-NPS-OA formulation showed the least effect of HF blockage on the skin permeation of Ibu compared to Ibu-Sol, Ibu-NPS and Ibu-NPS + OA (PM) (Fig. 6b).

In Vitro Drug Release from Nanoparticles

Controlled release of a drug from its delivery system is helpful for maintaining constant drug levels in the target tissues. During in vitro drug release studies, Ibu release from different nanoparticle formulations occured in a controlled manner (Fig. 7a). Ibu-NLC and Ibu-NLC-R11 showed $85 \pm 3\%$ release of Ibu within 24 h and followed Korsmeyer − Peppas release kinetics with a best fit r^2 value of 0.90. Similar to NLC, NPS showed an initial burst release followed by steady state release and approximately $86 \pm 6\%$ of the Ibu was released after 24 h (Fig. 7b) and followed Korsmeyer − Peppas kinetics with a best fit r^2 value of 0.93. Due to un-entrapped Ibu available in NLC and NPS dispersions, initial burst release of Ibu was observed. The drug released from surface modified and un-modified nanoparticles was statistically not different, due to use of a semipermeable membrane.

Cytotoxicity of Nanoparticles

The cytotoxicity of the nanoparticulate systems is a very important aspect to study. The safety profile of the surface modified and un-modified NLC and NPS was tested in the NHEK cells. The volume of applied tested formulation on the cells was maintained same as form the skin permeation studies. Un-modified nanoparticles (NLC and NPS) showed cell viability close to 100% against NHEK cells. Similarly, R11 and YKA modified NLC showed viability close to 100% indicating that the used concentration of CPPs is non-toxic to NHEK cells (Fig. 8). However, NPS-OA and NPS + OA (PM) showed cell viability of approximately 94–98% compared to NPS. This may be the result of OA interfering with the cellular membrane but overall viability was greater than $94 \pm 1.2\%$.

In Vivo Model for Allergic Contact Dermatitis (ACD)

The left ear thickness was same for the placebo formulations over the period of the therapy and hence the formulation excipients did not show any activity for the skin inflammation. The effect of DXM solution, Ibu-Sol, Ibu-NLC-R11 and Ibu-NPS-OA on the reduction of ear swelling is shown in Fig. 9a. The thickness of ears was increased from 140 ± 2 to 165 ± 5 µm for control (only DNFB treated) animals with increase in time, 0 to 72 h. After 72 h, the ear thickness was decreased to 86.89 µm, 49.56 µm and 38.63 µm for Ibu-Sol, Ibu-NLC-R11 and Ibu-NPS-OA, respectively. The DXM treated mice ears showed similar thickness before and after the treatment. The histological data from the study are illustrated in Fig. 9b. The inflammation treatments by Ibu-NLC-R11 and Ibu-NPS-OA formulations were then examined for cutaneous histology after 72 h of treatment. Compared to untreated control and Ibu-Sol treated ears, Ibu-NLC-R11 and Ibu-NPS-OA were highly effective in the treatment of ACD.
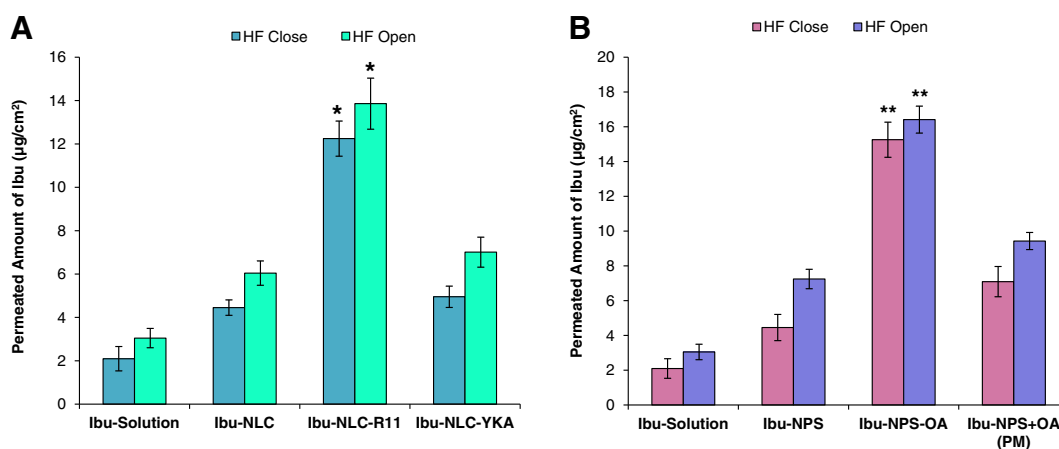

Fig. 6 Selective blocking of HF - Permeated amount of Ibu through the skin: The HF blocked and un-blocked test area of skin was evaluated for in vitro skin permeation for CPP and OA surface modified nanoparticles. The Ibu levels in the collected receiver compartment was evaluated at the end of 24 h (a) when applied as a form of CPP surface modified NLC and (b) when applied as a form of OA surface modified NPS. Data represent mean ± SD, n = 12, significance Ibu-NLC-R11 against Ibu-Sol, Ibu-NLC and Ibu-NLC-YKA, *p < 0.05; significance Ibu-NPS-OA against Ibu-Sol, Ibu-NPS and Ibu-NPS + OA (PM), **p < 0.05.
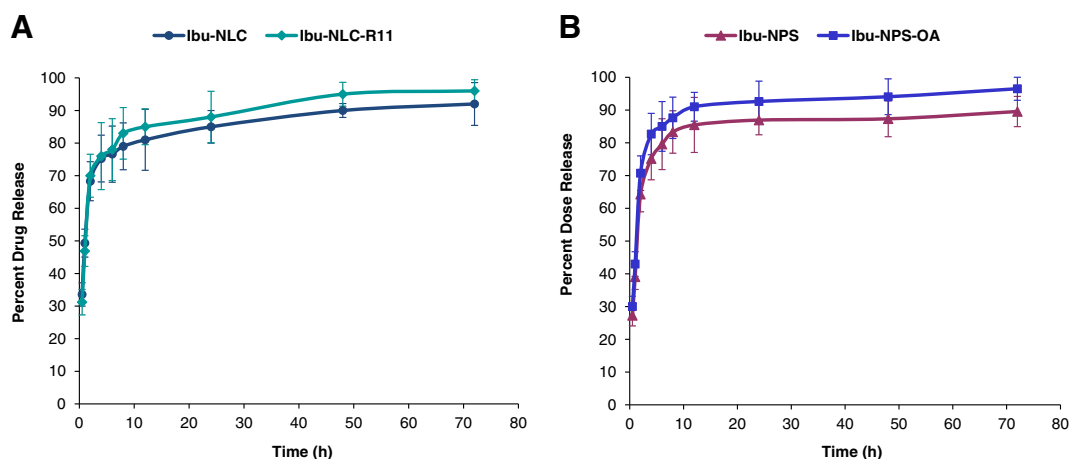
Fig. 7 *In vitro* drug release of (**a**) lipid nanoparticles: Ibu-NLC and Ibu-NLC-R11 and (**b**) polymeric nanoparticles: Ibu-NPS and Ibu-NPS-OA in PBS (pH 7.4) containing 0.1%w/v volpo 20. The cumulative amount released was plotted against time. *In vitro* drug release results show initial burst release followed by steady state release and after 72 h approximately 85–95% of the Ibu was released. The Data represent mean ± SD, $n = 6$.

DISCUSSION

In recent years, the penetration profile of lipid and polymeric nanoparticles has been of major interest among researchers (3,10–14). To enhance skin permeation of active drugs, we have developed two types of drug delivery systems: i) lipid based nanocarriers (NLC) tagged with CPP and ii) polymeric nanoparticles (NPS) tagged with OA. These systems showed significant improvement in the skin permeation of encapsulated drugs and thus, have the potential for enhancement in therapeutic response against inflammatory skin diseases (10–14). However, the mechanism involved in the skin permeation of these surface modified nanoparticles is unknown. Therefore, the present study focuses on investigation of penetration pathways of surface modified nanoparticles across the skin. There are mainly
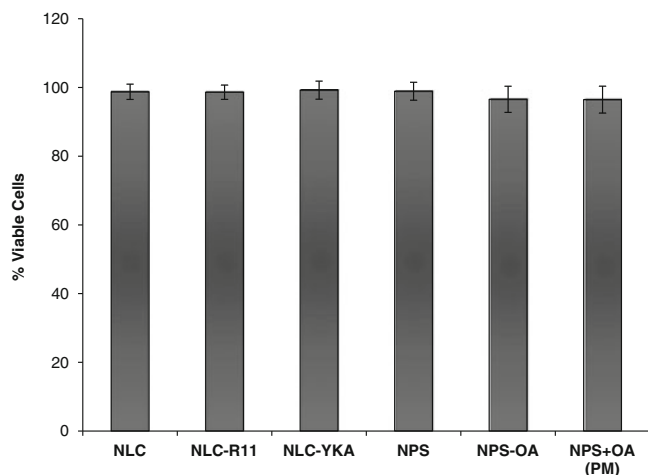

Fig. 8 Cytotoxicity of nanoparticles: The surface modified and unmodified NLC and NPS formulations (without drug) showed viability close to 100% against NHEK cells. The Data represent mean ± SD, $n = 6$.

three possible mechanisms by which CPPs and OA can enhance percutaneous transport of the drug molecules: 1) by structurally altering the lipids present in the intercellular region (intercellular pathway); 2) by disturbing the protein domain like the cross-linked keratin and keratinocytes other proteins (transcellular pathway) and 3) through hair follicles.

From decades, it is very well known that for percutaneous penetration of the permeant intercellular and/or intracellular pathway(s) plays a major role. Therefore, to investigate the skin penetration pathways of surface modified nanoparticles, we have used EpiDermFT™ cultures as an *in vitro* model. EpiDermFT™ cultures do not have HF and they consist of differentiated skin layers (SC, epidermis and dermis) similar to human skin. The confocal microscopy studies demonstrated distribution of fluorescence from DiO-NLC and DiO-NPS mainly in the SC (Fig. 1). However, DiO-NLC-R11 and DiO-NPS-OA showed significant increases in fluorescence throughout the epidermis and dermis. This is mainly due to the superior permeation-enhancing ability of R11 and OA which interact with either skin lipids (intercellular) or skin proteins (transcellular). These results were in agreement with earlier studies where CPPs like penetratin (31), TAT (32), R8 (32) and T2 (33) are reported to disturb structural orientation of lipid domains in the skin. Similarly, OA is known to create temporary defects within the lipid bilayers of SC and can leads to the enhanced drug permeation deep inside the skin (34).

In addition to non-follicular penetration pathways, the follicular penetration pathway has been shown to be of special relevance for nanoparticluate based skin delivery (7,8,35–37). It has been reported that nanoparticles below 600 nm can penetrate efficiently through the follicular pathway (38). In addition, the size and composition of the nanoparticles have an enormous influence on the follicular penetration process. In general, particles above 100 nm
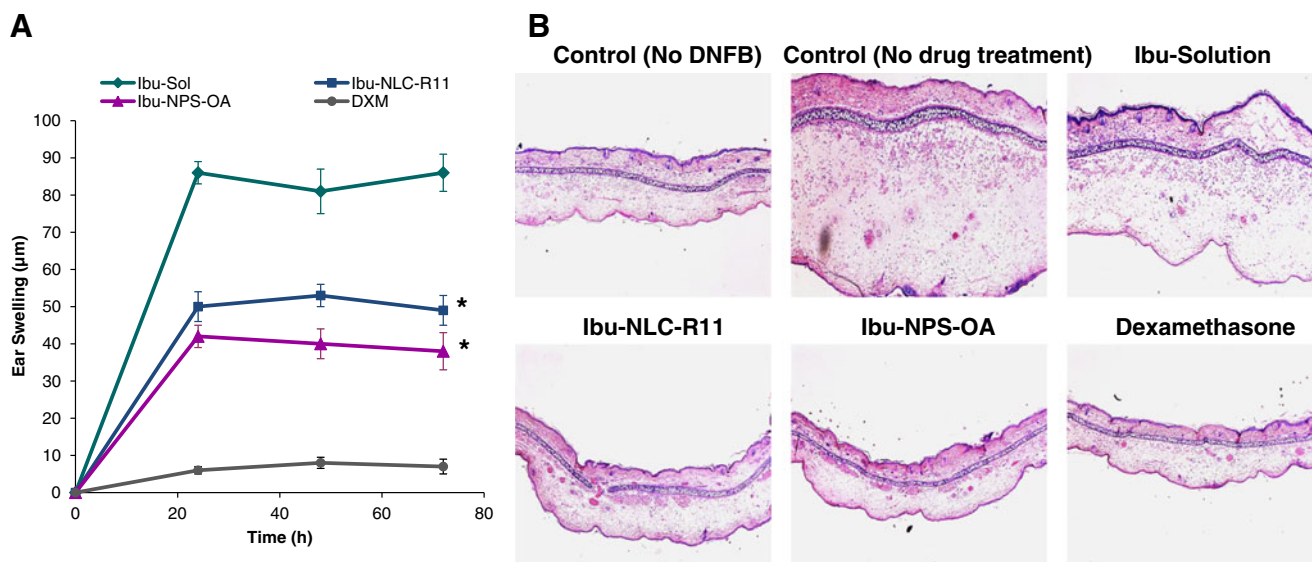
Fig. 9 (**a**) Effect of Ibu-Sol, surface modified nanoparticles containing Ibu and dexamethasone (DXM) on the reduction of ACD in C57/BL mice ears. Data represent mean ± SD, $n = 4$, significance Ibu-NLC-R11 and Ibu-NPS-OA against Ibu-Sol, $*p < 0.001$. (**b**) H&E staining of inflammation induced by topical application of DNFB, and after 72 h treatment Ibu-Sol, Ibu-NLC-R11 and Ibu-NPS-OA with a positive control, DXM.

are not able to overcome the intact skin barrier, neither the barrier of the SC nor HF (9). Here in the present study the nanoparticles size was in the range of 140–195 nm. Therefore, due to size restrictions, it was assumed that these nanoparticles are restricted into the upper layers of SC and HF. Besides particle size, another aspect of particulate delivery into HF is physicochemical properties such as surface charge and composition. Jung *et al.* (39) suggested that a cationic surface charge is helpful for follicular and non-follicular penetration assuming that skin and HF are negatively charged leading to the binding of the cationic particles in an ion-exchange manner. Our surface modified nanoparticles contain cationic surface charge in the case of NPS or NPS-OA and positively charged surface tags in the case of NLC-R11. This cationic charge may explain the enhanced Ibu penetration into the skin and into the receiver compartment in permeation studies.

To further differentiate between the intrafollicular and non-intrafollicular pathways, the amount of drug in SC, Epi + Derm and HF was assessed. Advanced measuring techniques are required to assess the follicular deposition and storage, which allow a differentiation between follicular and non-follicular drug penetration. In this study, the differential stripping technique was employed because it is more suitable for the investigation of drug retained in HF and SC. Differential stripping showed significantly higher amounts of Ibu present into HF for Ibu-NLC-R11 and Ibu-NPS-OA than respective controls (Fig. 2). The amount of Ibu retained in the SC reservoir was significantly higher than the HF reservoir for different nanoparticle formulations, suggesting that the HF may play a minor role in the penetration of these particles and thus, encapsulated drugs.

However, this observation may be due to the use of *in vitro* conditions (27). Patzelt *et al.* (21) observed that drug penetrated through and retained in the HF was higher for *in vivo* experiments compared to *in vitro* conditions. Therefore, to overcome the limitation of the differential stripping technique, selective blocking of HF technique was chosen for investigating the effect of hair follicle closure on the percutaneous delivery of drug encapsulated surface modified nanoparticles.

Trauer *et al.* (25) compared *in vivo* and *in vitro* penetration of caffeine into HF and suggested that the *in vitro* follicular closing technique is applicable to study the penetration pathways of active drugs. On the other hand, this technique requires specialized expertise (27). Therefore, to optimize this technique several attempts were made in our laboratory and prior to performing the current study, CLSM study was performed. CLSM data suggested that the optimized technique can selectively seal the opening of the HF (Fig. 4). Further, the skin permeation of nanoparticle formulations before and after HF closure (HF open and close) showed that the amount of Ibu permeated in receiver compartment and retained in skin was unaffected by HF closure. This is further supported from our differential stripping studies which were conducted with Ibu and HF blocked skin and the results suggested that the retention of Ibu in the SC, HF and Epi + Derm for HF closed and open skin were not significantly different (data not shown). This suggests that the follicular pathway plays a minor role in the skin permeation of Ibu encapsulated surface modified nanoparticles. In addition, the enhanced permeation of Ibu observed with the modified nanoparticles may be due to the interaction between lipid domains of SC and R11 or OA, present on the

surface of the nanoparticles. The results obtained with open and close HF are in agreement with the results of differential stripping technique. Similar observations are reported by Abdulmajed *et al.* (40), in which they found minor absorption through the HF in the permeation of retinyl ascorbate into porcine skin. Abdulmajed *et al.* applied tiny amounts of a water-resistant, fast0drying powder adhesive to seal porcine hair follicles selectively. Both HF closed and opened skin samples were then mounted on diffusion cells and retinyl ascorbate solution was topically applied. Drug deposition in the epidermis was evaluated by tape stripping and it was concluded that when the HF are intact they may not play a vital role in the epidermal permeation, however when the HF is disturbed (i.e. stretched) they can increase drug delivery into the skin by 20–40%. Thus, based on the results of the present study, we hypothesize that surface modified nanoparticles may follow these sequences of events: a) formation of a thin film on the SC after topical application of nanoparticles, b) enhancement of SC hydration and occlusion, c) adhesion of nanoparticles to the SC and HF cells (HF open) due to positive charge of nanoparticles, d) formation of permeability defects in lipid and protein strucures of SC due to contact of R11 and OA, e) release of encapsulated drug into the skin and HF where the drug can diffuse independently into deep skin layers. Moreover, the cytotoxicity assay of these surface modified nanoparticles against NHEK cells showed viability close to 100% (Fig. 8), signifying that the surface modified nanoparticles are non-toxic to normal skin cells.

Additionally, to explore the therapeutic efficacy of surface modified nanoparticles, allergic contact dermatitis (ACD) mouse model was used. Reduced inflammation was observed with the application of Ibu-NLC-R11 and Ibu-NPS-OA compared to Ibu-Sol (Fig. 9), indicating that an increased amount of drug at the inflamed site is responsible for improving therapeutic efficacy of Ibu. It is also suggested that incorporating Ibu in NLC-R11 and NPS-OA facilitates diffusion of Ibu through skin layers. These results are in agreement with the earlier studies with celecoxib (10) and ketoprofen (11,14).

CONCLUSION

By using CLSM, differential stripping and HF closure techniques, the amount of the drug penetrated into the SC and HF can be determined upon topical application. The results from the current study demonstrated that the surface modification of the nanoparticles with the penetration enhancers (peptide, R11 and non-peptide, OA) can facilitate the enhanced accumulation of the encapsulated drug in the SC and HF reservoirs, which can further reach therapeutic sites in the skin. In conclusion, R11 and OA modified

nanoparticles mainly deliver drug molecules into deep epidermis and dermis through non-follicular (major route) and follicular pathways (minor route).

REFERENCES

1. Meidan VM, Bonner MC, Michniak BB. Transfollicular drug delivery—is it a reality? Int J Pharm. 2005;306(1–2):1–14.
2. Lademann J, Richter H, Meinke M, Sterry W, Patzelt A. Which skin model is the most appropriate for the investigation of topically applied substances into the hair follicles? Skin Pharmacol Physiol. 2010;23(1):47–52.
3. Desai P, Patlolla RR, Singh M. Interaction of nanoparticles and cell-penetrating peptides with skin for transdermal drug delivery. Mol Membr Biol. 2010;27(7):247–59.
4. Mehnert W, Mader K. Solid lipid nanoparticles: production, characterization and applications. Adv Drug Deliv Rev. 2001;47(2–3):165–96.
5. Mundargi RC, Babu VR, Rangaswamy V, Patel P, Aminabhavi TM. Nano/micro technologies for delivering macromolecular therapeutics using poly(D, L-lactide-co-glycolide) and its derivatives. J Control Release. 2008;125(3):193–209.
6. Soppimath KS, Aminabhavi TM, Kulkarni AR, Rudzinski WE. Biodegradable polymeric nanoparticles as drug delivery devices. J Control Release. 2001;70(1–2):1–20.
7. Papakostas D, Rancan F, Sterry W, Blume-Peytavi U, Vogt A. Nanoparticles in dermatology. Arch Dermatol Res. 2011;303 (8):533–50.
8. Lademann J, Richter H, Teichmann A, Otberg N, Blume-Peytavi U, Luengo J, *et al.* Nanoparticles–an efficient carrier for drug delivery into the hair follicles. Eur J Pharm Biopharm. 2007;66(2):159–64.
9. Knorr F, Lademann J, Patzelt A, Sterry W, Blume-Peytavi U, Vogt A. Follicular transport route–research progress and future perspectives. Eur J Pharm Biopharm. 2009;71(2):173–80.
10. Desai PR, Shah PP, Patlolla RR, Singh M. Dermal Microdialysis Technique to Evaluate the Trafficking of Surface-Modified Lipid Nanoparticles upon Topical Application. Pharm Res. 2012;29 (9):2587–600.
11. Shah PP, Desai PR, Channer D, Singh M. Enhanced skin permeation using polyarginine modified nanostructured lipid carriers. J Control Release. 2012;161(3):735–45.
12. Patlolla RR, Desai PR, Belay K, Singh MS. Translocation of cell penetrating peptide engrafted nanoparticles across skin layers. Biomaterials. 2010;31(21):5598–607.
13. Shah PP, Desai PR, Patel AR, Singh MS. Skin permeating nanogel for the cutaneous co-delivery of two anti-inflammatory drugs. Biomaterials. 2012;33(5):1607–17.
14. Shah PP, Desai PR, Singh M. Effect of oleic acid modified polymeric bilayered nanoparticles on percutaneous delivery of spantide II and ketoprofen. J Control Release. 2012;158(2):336–45.

15. El Maghraby GM, Williams AC, Barry BW. Skin hydration and possible shunt route penetration in controlled estradiol delivery from ultradeformable and standard liposomes. J Pharm Pharmacol. 2001;53(10):1311–22.

16. Essa EA, Bonner MC, Barry BW. Human skin sandwich for assessing shunt route penetration during passive and iontophoretic drug and liposome delivery. J Pharm Pharmacol. 2002;54(11):1481–90.

17. Barry BW. Drug delivery routes in skin: a novel approach. Adv Drug Deliv Rev. 2002;54 Suppl 1:S31–40.

18. Grams YY, Bouwstra JA. A new method to determine the distribution of a fluorophore in scalp skin with focus on hair follicles. Pharm Res. 2002;19(3):350–4.

19. Grams YY, Whitehead L, Lamers G, Sturmann N, Bouwstra JA. On-line diffusion profile of a lipophilic model dye in different depths of a hair follicle in human scalp skin. J Invest Dermatol. 2005;125(4):775–82.

20. Teichmann A, Jacobi U, Ossadnik M, Richter H, Koch S, Sterry W, et al. Differential stripping: determination of the amount of topically applied substances penetrated into the hair follicles. J Invest Dermatol. 2005;125(2):264–9.

21. Patzelt A, Richter H, Buettemeyer R, Huber HJ, Blume-Peytavi U, Sterry W, et al. Differential stripping demonstrates a significant reduction of the hair follicle reservoir in vitro compared to in vivo. Eur J Pharm Biopharm. 2008;70(1):234–8.

22. Teichmann A, Ossadnik M, Richter H, Sterry W, Lademann J. Semiquantitative determination of the penetration of a fluorescent hydrogel formulation into the hair follicle with and without follicular closure by microparticles by means of differential stripping. Skin Pharmacol Physiol. 2006;19(2):101–5.

23. Trauer S, Lademann J, Knorr F, Richter H, Liebsch M, Rozycki C, et al. Development of an in vitro modified skin absorption test for the investigation of the follicular penetration pathway of caffeine. Skin Pharmacol Physiol. 2010;23(6):320–7.

24. Otberg N, Patzelt A, Rasulev U, Hagemeister T, Linscheid M, Sinkgraven R, et al. The role of hair follicles in the percutaneous absorption of caffeine. Br J Clin Pharmacol. 2008;65(4):488–92.

25. Trauer S, Patzelt A, Otberg N, Knorr F, Rozycki C, Balizs G, et al. Permeation of topically applied caffeine through human skin—a comparison of in vivo and in vitro data. Br J Clin Pharmacol. 2009;68(2):181–6.

26. Blume-Peytavi U, Massoudy L, Patzelt A, Lademann J, Dietz E, Rasulev U, et al. Follicular and percutaneous penetration pathways of topically applied minoxidil foam. Eur J Pharm Biopharm. 2010;76(3):450–3.

27. Meidan VM. Methods for quantifying intrafollicular drug delivery: a critical appraisal. Expert Opin Drug Deliv. 2010;7(9):1095–108.

28. Mallampati R, Patolla RR, Agarwal S, Babu RJ, Hayden P, Klausner M, et al. Evaluation of EpiDerm full thickness-300 (EFT-300) as an in vitro model for skin irritation: studies on aliphatic hydrocarbons. Toxicol In Vitro. 2010;24(2):669–76.

29. Teichmann A, Otberg N, Jacobi U, Sterry W, Lademann J. Follicular penetration: development of a method to block the follicles selectively against the penetration of topically applied substances. Skin Pharmacol Physiol. 2006;19(4):216–23.

30. Chougule MB, Patel AR, Jackson T, Singh M. Antitumor activity of Noscapine in combination with Doxorubicin in triple negative breast cancer. PLoS One. 2011;6(3):e17733.

31. Cohen-Avrahami M, Libster D, Aserin A, Garti N. Sodium diclofenac and cell-penetrating peptides embedded in H(II) mesophases: physical characterization and delivery. J Phys Chem B. 2011;115(34):10189–97.

32. Afonin S, Frey A, Bayerl S, Fischer D, Wadhwani P, Weinkauf S, et al. The cell-penetrating peptide TAT(48–60) induces a non-lamellar phase in DMPC membranes. Chemphyschem. 2006;7(10):2134–42.

33. Kumar S, Sahdev P, Perumal O, Tummala H. Identification of a novel skin penetration enhancement peptide by phage display peptide library screening. Mol Pharm. 2012;9(5):1320–30.

34. Rowat AC, Kitson N, Thewalt JL. Interactions of oleic acid and model stratum corneum membranes as seen by 2H NMR. Int J Pharm. 2006;307(2):225–31.

35. Mak WC, Patzelt A, Richter H, Renneberg R, Lai KK, Ruhl E, et al. Triggering of drug release of particles in hair follicles. J Control Release. 2012;160(3):509–14.

36. Patzelt A, Richter H, Knorr F, Schafer U, Lehr CM, Dahne L, et al. Selective follicular targeting by modification of the particle sizes. J Control Release. 2011;150(1):45–8.

37. Vogt A, Combadiere B, Hadam S, Stieler KM, Lademann J, Schaefer H, et al. 40 nm, but not 750 or 1,500 nm, nanoparticles enter epidermal CD1a + cells after transcutaneous application on human skin. J Invest Dermatol. 2006;126(6):1316–22.

38. Wosicka H, Cal K. Targeting to the hair follicles: current status and potential. J Dermatol Sci. 2010;57(2):83–9.

39. Jung S, Otberg N, Thiede G, Richter H, Sterry W, Panzner S, et al. Innovative liposomes as a transfollicular drug delivery system: penetration into porcine hair follicles. J Invest Dermatol. 2006;126(8):1728–32.

40. Abdulmajed K, Heard CM. Topical delivery of retinyl ascorbate. 3. Influence of follicle sealing and skin stretching. Skin Pharmacol Physiol. 2008;21(1):46–9.